Helix Rotation Model of the Flagellar Rotary Motor

Rüdiger Schmitt
Institute of Biochemistry, Genetics, and Microbiology, University of Regensburg, D-93040 Regensburg, Germany

ABSTRACT A new model of the flagellar motor is proposed that is based on established dynamics of the KcsA potassium ion channel and on known genetic, biochemical, and biophysical facts, which accounts for the mechanics of torque generation, force transmission, and reversals of motor rotation. It predicts that proton (or in some species sodium ion) flow generates short, reversible helix rotations of the MotA-MotB channel complex (the stator) that are transmitted by Coulomb forces to the FliG segments at the rotor surface. Channels are arranged as symmetric pairs, S and T, that swing back and forth in synchrony. S and T alternate in attaching to the rotor, so that force transmission proceeds in steps. The sense of motor rotation can be readily reversed by conformationally switching the position of charged groups on the rotor so that they interact with the stator during the reverse rather than forward strokes. An elastic device accounts for the observed smoothness of rotation and a prolonged attachment of the torque generators to the rotor, i.e., a high duty ratio of each torque-generating unit.

INTRODUCTION

Bacteria swim by rotating their helical flagella (Berg and Anderson, 1973; Silverman and Simon, 1974). The rotary motor at the flagellar base is located in the cell envelope (DePamphilis and Adler, 1971), it is encircled by 8–16 force-generating units (Block and Berg, 1984; Blair and Berg, 1988; Khan et al., 1988; Muramoto et al., 1994), and it is energized by a H^+ (or in some species Na^+) gradient across the cytoplasmic membrane (Manson et al., 1977; Hirota et al., 1981). Each revolution consumes ≈1000 H^+ (Meister et al., 1987) and requires ≈400 steps (Samuel and Berg, 1995). The bacterial flagellar motor is thus a molecular machine, which converts electrochemical energy into mechanical work.

The overall organization of a flagellum (as drawn in Fig. 1) and many structural and functional details have been elucidated (for review see Macnab, 1996; Berg, 2003). The thin helical filament (propeller) joins the flagellar basal body via a flexible hook (universal joint) that is connected to a straight rod (drive shaft). The rod is held by two rings in the cell envelope and is firmly connected to the MS ring (composed of FliF protein) located in and just outside of the cytoplasmic membrane. The motors of most motile species studied reverse the sense of rotation, whereas the motors of some rotate unidirectionally but can adjust their rotary speed (Götz and Schmitt, 1987; Platzer et al., 1997; Schmitt, 2002) or follow a stop-and-go pattern of rotation (Armitage and Macnab, 1987; Armitage and Schmitt, 1997). The motor-switch complex is firmly attached to the MS ring as a bell-shaped structure known as the C ring. The complex contains two proteins (FliM and FliN) and a third (FliG) that connects the C and MS rings. These components are involved in the generation of torque and switching of direction and are believed to rotate along with the MS ring, rod, hook, and filament. The MS ring is made up of 26 ± ≈2 subunits of FliF (Jones et al., 1990; Sosinsky et al., 1992; Thomas et al., 1999), and the inferred 1:1 FliF/FliG stoichiometry suggests the presence of an equal number of FliG subunits in the motor. FliG is, thus, an extended portion of the MS ring.

The stator is composed of two transmembrane proteins, MotA and MotB (PomA and PomB in Na^+ driven flagella; Hirota et al., 1981), that surround the MS ring. Four transmembrane helices of MotA and one amino-terminal, hydrophobic helix of MotB form a proton channel through the cytoplasmic membrane, and the carboxy-terminal, periplasmic domain of MotB is probably anchored to the cell wall (Macnab, 1996; Berg, 2003). Torque generation has been shown to involve electrostatic interactions between the C-terminal domain of FliG (rotor) and the cytoplasmic domain connecting the transmembrane helix segments *2* and *3* of MotA (stator) (Zhou et al., 1998a) in response to an inward H^+ flow. This observation has a central role in the model proposed here.

Although many details of the flagellar motor structure have been elucidated, the mechanism by which the transmembrane flow of H^+ (or Na^+) is coupled to flagellar rotation is not understood. A variety of models have been proposed (for review see Berg and Turner, 1993; Berry and Armitage, 1999) that postulate fixed elastic elements linking the stator to the cell wall (Berg and Khan, 1983), acting as cross-bridges between stator and rotor (Oosawa and Hayashi, 1983; Läuger, 1988), or operating by electrostatic interaction (Berry, 1993; Elston and Oster, 1997; Walz and Caplan, 2000). The majority of these models treat stator elements as fixed units that convert energy either by Coulomb forces or by ''channeling'' the H^+ flow (Berg and Khan, 1983). Where conformational changes of the stator have been postulated (Oosawa and Hayashi, 1983; Läuger, 1988; Atsumi, 2001), these involve fixed elements similar to muscle cross-bridges, a feature not supported by fine-structure analyses. Unlike these models, the concept of

Submitted March 10, 2003, and accepted for publication May 6, 2003.

Address reprint requests to Dr. Rüdiger Schmitt, Lehrstuhl für Genetik, University of Regensburg, D-93040 Regensburg, Germany. Tel.: 49-941-9433162; Fax: 49-941-9433163; E-mail: rudy.schmitt@biologie.uni-regensburg.de.

0006-3495/03/08/843/10 $2.00

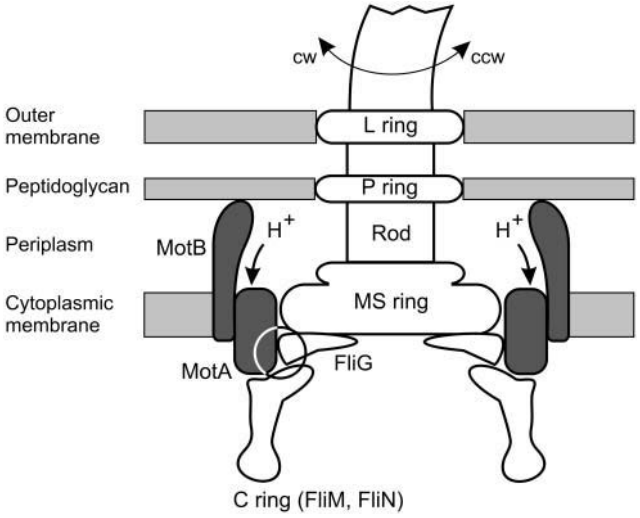

FIGURE 1 Schematic view of the flagellar basal body imbedded in the cell envelope of a Gram-negative bacterium. The central part (*white*) rotates, whereas the torque-generating MotA-MotB proton channels (*dark shading*) are anchored to the peptidoglycan layer of the cell envelope (*gray*). Torque is generated by the flow of protons (H^+) across the cytoplasmic membrane via MotA-MotB and by interactions between MotA (stator) and FliG (rotor) (*circled portion*). Most flagellar motors reverse the sense of rotation from counterclockwise (*ccw*) to clockwise (*cw*), although some rotate unidirectionally cw and modulate rotary speed (Schmitt, 2002).

Blair and his colleagues predicts a conformational change in the stator that pushes the rotor through a small angle (Kojima and Blair, 2001), either by electrostatic interaction or by direct contact (Braun et al., 1999). These latter models share the concept of a flexible stator element with the model proposed here. The present model diverges from other models by proposing that rotational movements are generated by reversible helix rotation of the stator elements. It predicts that these rotational movements are transmitted to the rotor by electrostatic coupling. The model takes into explicit account a number of structural and functional facts, including bidirectionality, smoothness of rotation, and a high duty ratio of the torque-generating units (Ryu et al., 2000; Berg, 2003).

MODELING

Requirements of a satisfactory model

Any proposed model for the flagellar motor has to consider i), the structural elements responsible for energization and rotation of the motor; ii), the nature of the forces acting between stator and rotor; and iii), the mode of energy conversion from an electrochemical gradient to mechanical work. I will begin by defining these three aspects.

i. Electron microscopic, biochemical, and genetic studies have established the motor geometry (Francis et al., 1994; Macnab, 1996) that is shown schematically in Fig. 1. The energy-transducing elements consist of the MS ring (FliF protein) with 26 ± 2 copies of FliG attached to its cytoplasmic face constituting the rotor, and the 8–16 MotA-MotB H^+ conducting transmembrane channels constituting the stator (Blair and Berg, 1988; Khan et al., 1988). Whereas FliG has previously been assigned to the C ring, its intermediate location and an apparent 1:1 FliG/FliF stoichiometry (26 ± 2 subunits each) argue for its allocation to an extended MS ring (Francis et al., 1992; Thomas et al., 1999, 2001).

ii. Systematic mutational analyses of motile *Escherichia coli* by Blair and his colleagues (Lloyd and Blair, 1997; Zhou et al., 1998a) demonstrated that charged residues in both the C-terminal portion of FliG (rotor) and in the cytoplasmic domain connecting transmembrane helices *2* and *3* of MotA (stator) are essential for motor function. Double mutants in which the conserved charged residues were replaced by either neutral or opposite-charge residues identified a number of interacting residues on the two proteins that are essential for torque generation. Based on patterns of synergism and suppression, the data suggested that Asp^{288} and Asp^{289} on FliG interact with Arg^{90} on MotA, and that Arg^{281} on FliG interacts with Glu^{98} on MotA. Moreover, clustering of the functionally important charged residues along a prominent ridge of the C-terminal domain of FliG recommends FliG subunits as the part of the rotor that interact with the stator (Lloyd et al., 1999). Directed mutagenesis of MotB and controlled proteolysis of MotA indicated that a conserved Asp^{32} residue of MotB is the principal proton-binding site that also directs conformational changes of MotA (Zhou et al., 1998b; Kojima and Blair, 2001). Like two essential proline residues of MotA, Asp^{32} is located at the cytoplasmic end of a membrane-spanning domain. Together, these three residues are thought to form a site that controls the conformation of the stator in a protonation-mediated fashion (Braun et al., 1999). In suggesting that protons flow through the MotA-MotB channel without binding to sites on the rotor, these data exclude a number of models that postulate the direct interaction of force-generating protons with the rotor.

iii. The mechanism by which electrochemical energy is transformed to mechanical work in the flagellar motor has been a persistent enigma. One essential feature of the concept proposed here relates to the mode of energy conversion that takes place in the stator. I propose that ion conductance through the H^+ channel serves to directly transform the electrochemical gradient into rotary motion. Therefore, instead of being fixed, the stator is considered a dynamic device. In their ''turbine model,'' Elston and Oster (1997) also postulate a ''movable stator,'' but this term just refers to a certain amount of freedom in the stator to move passively. I visualize active movement within the stator.

A dynamic-stator model

How can we envisage such stator movements? Without crystal-structure details for the flagellar MotA-MotB H^+ channel, I have drawn an analogy to the ubiquitous KcsA K^+ channel (Schrempf et al., 1995), the first ion channel whose crystal structure was solved (Doyle et al., 1998; Zhou et al., 2001). The KcsA channel is a tetramer with four outer (TM1) and four inner (TM2) transmembrane helices, the latter forming the K^+ conducting pore with a selectivity filter. Perozo et al. (1999) applied targeted spin labeling and electron paramagnetic resonance (EPR) spectroscopy to study pH-induced gating of the KcsA channel. Their central conclusion was that gating is accompanied by conformational changes of TM1 and TM2, namely, rigid-body translations and counterclockwise rotations around the channels central cavity, as the pore opens. In keeping with these authors, the top-view model in Fig. 2 *A* illustrates a rotational displacement of the four TM2 helices that opens the permeation pathway. Gating of the KcsA channel is a fast process, and reversals occur in $\sim 10^{-10}$ s. By analogy, the five transmembrane helices of the MotA-MotB H^+ channel viewed from the cytoplasmic face are proposed to form a rotating pentamer, as diagrammed in Fig. 2 *B*. The MotA membrane-spanning helices *2* and *3* are linked by the ~120-residue cytoplasmic domain that contains the charged residues Arg^{90} and Glu^{98} symbolized as "+" and "−," respectively, which are considered to be essential for electrostatic force transmission to the rotor (Zhou et al., 1998a). As in Fig. 2 *A*, the channel opens by counterclockwise rotation of the five transmembrane helices, causing a concurrent movement of the cytoplasmic domain with its charged residues. Opening and closing of the MotA-MotB H^+ channel—like that of the KcsA channel—proceeds in a reversible fast-kinetic fashion.

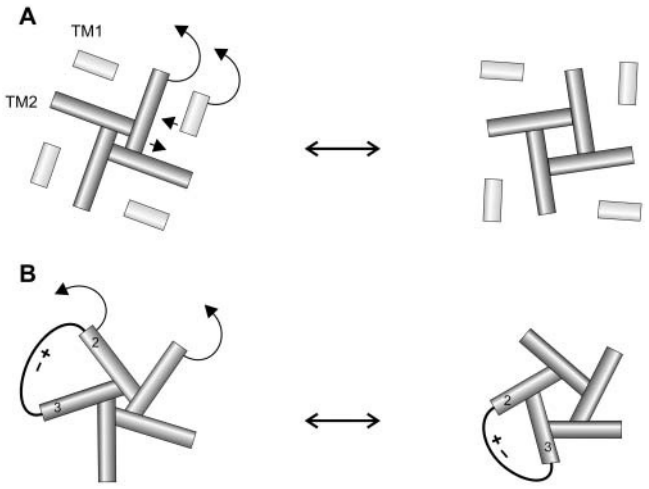

FIGURE 2 Helix rotation as the proposed molecular mechanism of gating in the KcsA K^+ (*A*) and the flagellar MotA-MotB H^+ channels (*B*). (*A*) Top view of KcsA in closed (*left*) and open (*right*) conformation deduced from crystal structure information (Doyle et al., 1998; Zhou et al., 2001) combined with site-directed spin labeling and electron paramagnetic resonance spectroscopy according to Perozo et al. (1999). Four outer transmembrane helices (*TM1*) and four inner helices (*TM2*) rotate (*bent arrows*) and tilt (*straight arrows*) relative to one another, when switching from the closed to the open conformation (H^+-induced gating). In the native channel, reversals follow fast kinetics in the 10^{-10}-s range. (*B*) Proposed mechanism of gating in the MotA-MotB H^+ channel. The model is viewed from the cytoplasmic side of the membrane. Four transmembrane helices of MotA and one of MotB are represented as cylinders forming the channel (*center*). The cytoplasmic loop containing the functional residues, R90(+) and E98(−), is shown as an arc connecting helices *2* and *3* of MotA. In analogy to *A*, transmembrane helices rotate in ccw direction and away from the central H^+ permeation pathway to open the channel. Charged residues on the polypeptide loop being pulled by the movement of adjacent helices *2* and *3* follow the rotation of the helix ends around the center of the channel (*bent arrows*). In H^+ channels driving the flagellar rotor, reversal kinetics range between 10^{-4} and 10^{-5} s.

In summary, my model postulates that i), H^+ (or Na^+) ions are conducted through the MotA-MotB (or PomA-PomB) channels and not along the rotor-stator interface; ii), the flow of H^+, driven by the proton motive force (pmf), is accompanied by reversible rotational movements of the transmembrane helices that form the ion channel; and iii), these rotational movements include the cytoplasmic domain of MotA that contains charged residues that are needed for force transmission to the rotor.

Force transmission from stator to rotor

In the present model, the conversion of electrochemical energy into rotational movements takes place in the stator elements, and then rotation is transmitted to the rotor by Coulomb forces acting between antipodal pairs of charged residues. The proposed interaction is illustrated in Fig. 3 by a top-view diagram that depicts two successive phases of the stator-rotor interaction. A FliG subunit, drawn as a segment of the large circular rotor and bearing at its periphery −/+ charges (only two shown for simplicity) faces the cytoplasmic domain of MotA (with antipodal +/− charges) drawn as part of the cylindrical stator element. Force is transmitted from the stator to the rotor by electrostatic interactions between the antipodal charged residues facing each other. In this scheme (Fig. 3, *top*), one power stroke of the stator turns the rotor by half a segment. In accordance with reversible helix rotation (Fig. 2), the stator swings back (in absence of any electrostatic contact with charges at the rotor face) and assumes its original configuration (Fig. 3, *bottom*). It is important to note that the stator domain reverses in a slightly different plane, thereby avoiding contact with its charged antipodes on the rotor periphery. This aspect is essential for explaining both sustained unidirectional rotation and rapid switching of the direction of rotation (see below).

The electrostatic interaction at the rotor-stator interface deserves a bit of additional consideration. As the stator turns counterclockwise (ccw), it rotates the rotor clockwise (cw) as

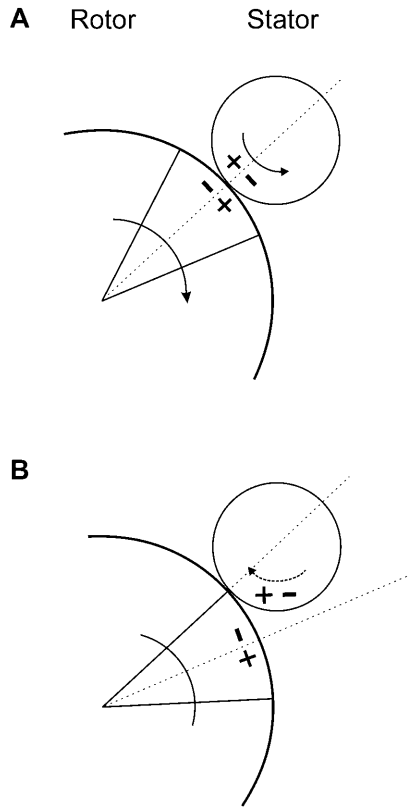

FIGURE 3 Diagram illustrating helix rotation of one channel (*stator*) and electrostatic force transmission to the rotor. (*A*) The rotor (*arc*) with one FliG subunit symbolized by a segment interacting with one MotA-MotB stator element (*circle*). Charged residues (only two are drawn for simplicity) at the FliG rim and in the cytoplasmic loop of MotA (Fig. 2) face each other in an antipodal configuration that facilitates electrostatic interaction. Small and large arrows indicate concurrent rotational movements of the stator and the rotor due to electrostatic coupling. (*B*) The rotor has been turned by half a FliG segment and the stator swings back (*stippled curved arrow*) without contacting antipodal charges at the rotor face (see text).

far as the interaction of Coulomb forces permits. Coulomb force F is defined by the equation

$$F = q_1 \times q_2 / r^2 \times D,$$

where q_1 and q_2 define a pair of interacting charges, r their separation, and D the dielectric constant of the medium. In biological systems, the value of D is critical for any model that relies on electrostatic interactions. The dielectric constant of water is 80, and that of a nonaqueous hydrophobic medium is ~2. Therefore, electrostatic forces are ~40-fold stronger in hydrophobic than in aqueous environments. For efficient force transmission, it is thus important that the rotor-stator interface be located in a quasi-water-free cavity close to the cytoplasmic membrane. This consideration is supported by electron micrographs, which locate the FliG subunits that are attached to the cytoplasmic surface of the MS ring and, by implication, the site of electrostatic interaction of FliG with MotA, at the inner surface of the cytoplasmic membrane (Francis et al., 1992; Thomas et al., 2001). Electron micrographs also suggest that the interactive sites may be sheltered from the aqueous cytoplasm by the protruding, bell-shaped C ring (as diagrammed schematically in Fig. 1; Francis et al., 1994). Alternatively, the rotor and stator proteins could be so designed as to create an interface from which water is largely excluded to secure strong electrostatic interactions in a low-dielectricity environment. However, Zhou et al. (1998a), in analyzing certain charged-residue mutants of MotA and FliG, report an impairment of motor function at higher ionic strength. This suggests at least some access of water to the interacting site. However, a dielectric constant of 40 (D = 40)—halfway between water and lipid—may be tolerated in the light of Berg's (2003) estimate of the force applied to the rotor. By assuming an average torque of 4000 pN nm generated by the force-generating units of the flagellar motor acting at the periphery of a rotor of radius 20 nm, he arrives at an applied force of 200 pN. By postulating eight independent force-generating units, one calculates that the contribution of each is 25 pN. This force equals in magnitude that between two electrons 4.8 Å apart in a medium of D = 40. It is, therefore, reasonable to assume that electrostatic interactions between the rotor and stator elements take place at a charge separation of no more than 4.8 Å, in an environment tolerating water molecules up to $D = 40$.

Two H^+ channels in one stator complex

Insights into the topology of the stator complex are essential for any model of the flagellar motor. A simple, sequence-derived membrane topology of the channel constituents MotA (transmembrane helices *1–4*) and MotB (helix *5*) is shown schematically in Fig. 4 *A*. However, a MotA:MotB complex with a stoichiometry of 4:2 has been recently supported by the following two kinds of biochemical evidence: i), Sizing chromatography of the reconstituted PomA-PomB Na^+ channel (the *Vibrio* homolog of the MotA-MotB H^+ channel) revealed an apparent mass consistent with a $(PomA)_4(PomB)_2$ stoichiometry (Sato and Homma, 2000); ii), Disulfide-cross-linking studies indicated that the α-helical transmembrane segments of two MotB subunits form a symmetric dimer in the MotA-MotB complex (Braun and Blair, 2001). These cross-linking patterns suggested an orientation of the two critical Asp^{32} residues away from the interface, so that they might function in two distinct H^+ channels. These studies also revealed some degree of rotational freedom (up to 40°) around the long axis of each α-helical segment of MotB. Consistent with the results of sizing chromatography, new cross-linking data point to a symmetric structure consisting of a central MotB dimer surrounded by four MotA subunits, each with four transmembrane segments (D.F. Blair, personal communication). Although the arrangement of four MotA subunits in two channels remains to be defined experimentally, the above results strongly support a model with symmetric pairs

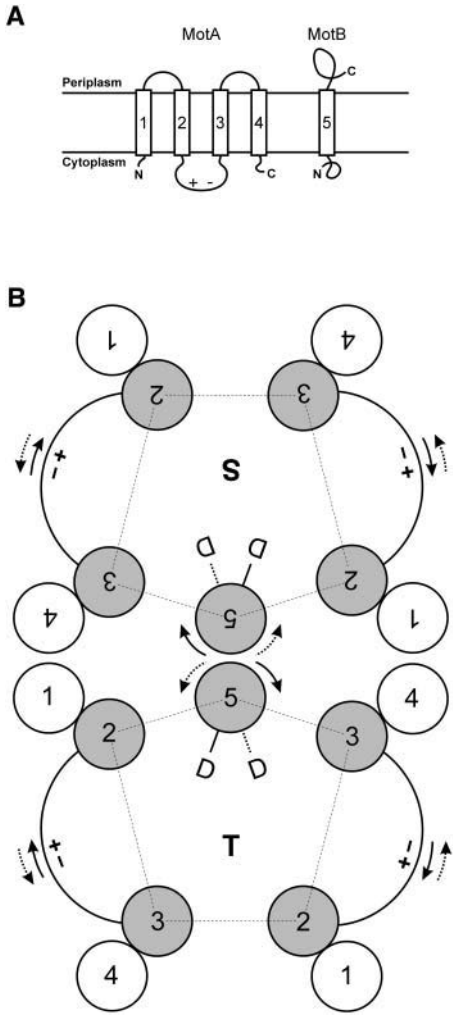

FIGURE 4 (*A*) Membrane topology of MotA (transmembrane helices *1–4*) and MotB (helix *5*). (*B*) Working model of the $(MotA)_4(MotB)_2$ complex (viewed from cytoplasm) postulating two pentameric H^+ channels, S and T, linked by a central MotB dimer. Each channel consists of a single MotB transmembrane helix (*5*) and eight MotA helices arranged as four inner (*2, 3*; *shaded*) and four outer (*1, 4*) helices derived from two MotA molecules. Four charge-bearing cytoplasmic domains that connect helices *2* and *3* are arranged pairwise on opposite faces of the dimeric complex, but only the two domains on one face act in force transmission to the rotor, whereas the pair on the opposite face is void (see text). The dimeric MotB helices (*5*) each contain a protonatable Asp^{32} residue (*D*) positioned in a way such that each can function in a different channel. Pmf-driven opening and closing (gating) of the binary channel causes inverse rotational movements of the two MotB helices (as illustrated by the two extreme positions of *D*; Braun and Blair, 2001) and concurrent rotations of the MotA helices in each channel including the charge-bearing domains (see Fig. 2). These forward and reverse rotations of S and T are illustrated by solid and dashed curved arrows, respectively.

of stator elements that have sufficient motional freedom to permit helix rotation.

A top view of the two-channels-in-one-complex concept has been diagrammed in Fig. 4 *B*, assuming a $(MotA)_4$ $(MotB)_2$ stoichiometry. The two pentameric H^+ channels, S and T, form an inverse-symmetrical pair that is linked by dimerization of MotB α-helices, each with a protonatable Asp^{32} residue. Each channel consists of one MotB (helix *5*) and eight MotA transmembrane helices arranged as four inner (helices *2* and *3*) and four outer (helices *1* and *4*) segments. This arrangement of the MotA transmembrane helices also permits a head-to-tail (*4* $\rightarrow$ *1*) fusion of two MotA subunits that has been shown (in the PomA homolog) to yield a mutant still capable of swimming (Sato and Homma, 2000). Four cytoplasmic domains connecting transmembrane helices *2* and *3* and containing the critical charges are arranged in pairs on opposite faces of the stator complex. In the present model only one pair of charged domains located on one face of the complex participates in force transmission to the rotor, whereas the pair on the opposite face remains void of such contacts. Conceivably, this twofold symmetry is necessary for assembling the stator complex around the rotor to secure a functional orientation of one set of force-transmitting domains toward the rotor periphery.

I propose that conformational changes by protonation/deprotonation of Asp^{32} (Kojima and Blair, 2001) mediate brief inverse rotations of the dimeric MotB helices (Braun and Blair, 2001) concurrent with rotation of the MotA helices and their critical cytoplasmic domains. Driven by the H^+ flow, the pair of channels reverses between two conformations and thus converts proton motive force into torque, involving oscillating rotations of the charge-bearing MotA domains (*bent arrows*, Fig. 4 *B*). These rotational movements are then transmitted electrostatically to the rotor (Fig. 3).

Model of the flagellar motor

The model shown in Fig. 5 consists of a rotor with 24 FliG segments encircled by 8 stator complexes, each of which consists of a pair of S and T elements. S and T rotate back and forth in synchrony (see Fig. 4) driven by protons moving through the complex. Due to the symmetry mismatch between 16 stator and 24 rotor elements, S and T alternate in moving the rotor. In the diagram (Fig. 5), torque is generated by the 8 S elements that match and electrostatically interact with 8 FliG segments. This pulls the rotor through half of a FliG segmental arc (or 7.5°) in the cw direction, and places the T stator elements into match position with FliG. Both S and T reverse without contacting antipodal charges and then T elements take over to pull the rotor around another 7.5°, as diagrammed in Fig. 6 (*left series*). One full turn of the rotor thus requires 24 power strokes of each of the 16 stator elements or $16 \times 24 = 384$ steps. This figure compares favorable with the ~400 steps per revolution deduced from electro-rotation experiments (Samuel and Berg, 1995). Given a maximal flagellar rotary speed of 300 Hz (Berg and Turner, 1993), and assuming tight energetic coupling of 2×24 rotational

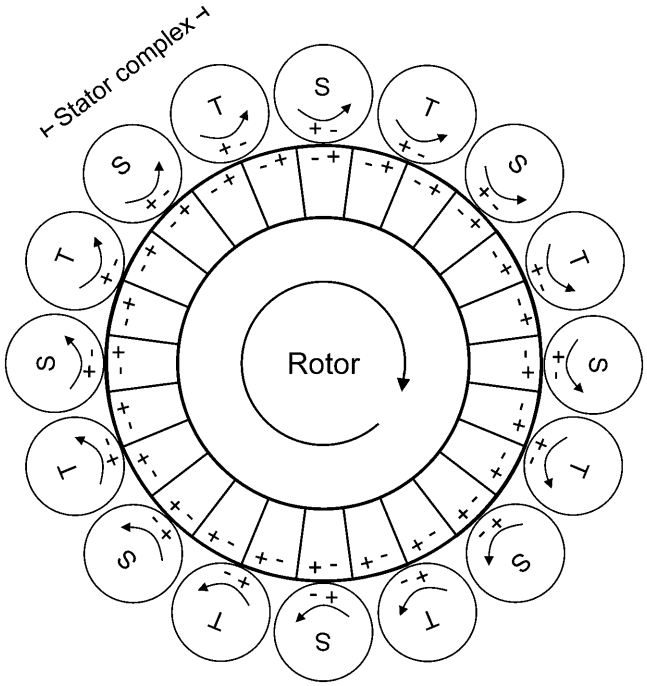

FIGURE 5 Model of the flagellar rotor with 24 radially arranged copies of FliG (segments) surrounded by 16 stator elements (H^+ channels) arranged as 8 S-T pairs (stator complexes). The two elements of a stator complex undergo brief rotational movements in a coordinate mode (*curved arrows*), as protons pass through the channels. At any given moment, one set (*S* in this scheme) interacts with the apposed rotor segment by antipodal charges and turns the rotor 1/48th of its circumference (half a segment) as shown in Fig. 3. Then the stator complex swings back (as in Fig. 3) without contacting antipodal charges at the rotor face, and brings the T set of elements into position ready to carry out the next step. Each of the 16 stator elements takes 24 productive and 24 unproductive turns, before one revolution of the rotor is completed.

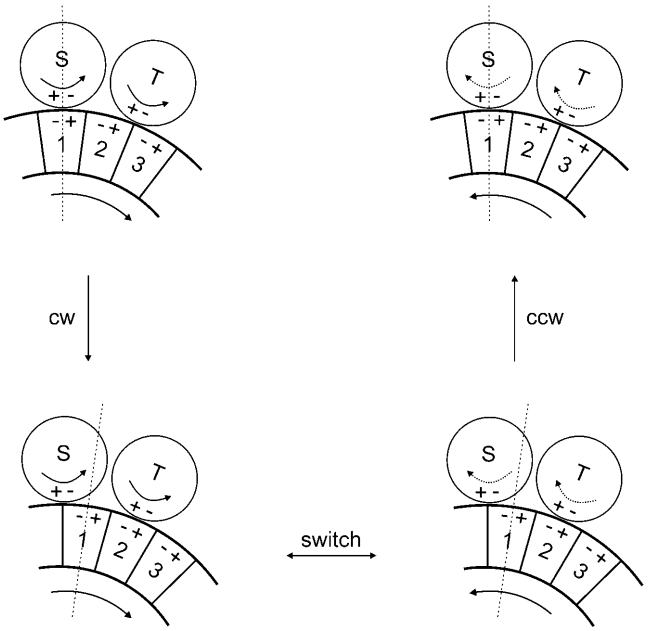

FIGURE 6 Rotor-stator relationships in clockwise (*left*) and counterclockwise (*right*) rotary progression, with alternation between these states indicated by the arrow labeled ''switch.'' In this scheme, oscillations of the force-generating stator elements, S and T, can be used to drive the rotor in either a cw or a ccw direction, depending on the conformational state of the rotor. The switch involves tilting of the FliG ramp into a position that will engage with either forward (*left*) or reverse (*right*) oscillations of the stator elements. Dotted lines indicate the amount of rotation (that results from one stroke of the stator elements).

movements of 1 stator element along with its rotor counterparts, the kinetics of conformational transitions range between 10^{-4} and 10^{-5} s.

The proposed model offers a convenient mechanism for switching the sense of motor rotation, provided that both forward and reverse rotational movements of the stator can be engaged in driving the rotor. As outlined above, in swinging back and forth, the charge-bearing stator domain moves along different latitudes with respect to the rotor edge, so that antipodal charges at the rotor-stator interface match in only one direction, not in the other. However, a match with the stator in its reverse beat (which will turn the rotor in the opposite direction) can be brought about by a conformational switch of the C ring that is believed to occur in the linker region of the FliG subunits (Brown et al., 2002). Fig. 6 illustrates the succession of rotor-stator interactions in the cw (*left*) and ccw (*right*) modes of rotation, and it outlines how a change of rotor conformation switches the system into the opposite rotational mode. Hence, conformational switching of the C ring tilts the rotor periphery into a position where it will match with either forward or backward rotating stator elements, so that bidirectionality becomes a direct consequence of reversible stator movements.

In most motile bacteria, reversals of flagellar rotation are the cause for changing the swimming direction, which is mandatory for tactic responses (Macnab, 1996). The present model adds a new twist to the discussion of how motor reversals are brought about.

A mechanical spring

A motor consisting of single force-generating units ought to generate torque in distinct increments, or steps. From a variance analysis of fluctuations in the rotation speed (inferring a stochastic behavior of the motor), it has been deduced that each revolution includes ~400 steps (Samuel and Berg, 1995). However, all direct measurements of flagellar rotation have failed to demonstrate a stepping motor. The failure to observe single steps has been attributed to intrinsic features, such as torsional elasticity of the flagellar hook in tethering experiments, or to many parallel torque-generating units working together. However, smoothness of rotation may equally well be intrinsic to the motor mechanism. Another feature of the torque-generating units is their high duty ratio (close to 1) observed in single flagella rotating under a varying load, which suggests that each

force-generating unit may be attached to the rotor for most of its mechanochemical cycle (Ryu et al., 2000; Berg, 2003).

Based on these qualities of the flagellar motor, I have introduced an elastic element into the model. Force transmission by elastic linkages has been considered early on by Berg and his colleagues (Berg and Anderson, 1973; Berg and Khan, 1983). I postulate that each cytoplasmic MotA domain with the driving charged residues (Fig. 4) acts like a mechanical spring. The action of the spring is directed by rotational movements of the MotA transmembrane helices *2* and *3* to which it is connected (Fig. 7). Its function in one power-stroke cycle is described by four consecutive steps. The springlike domain attaches to the rotor by electrostatic forces interacting between antipodal charges (Fig. 7 *A*). As the transmembrane helices *2* and *3* carry out their ccw rotation, the spring first expands, thus converting kinetic into potential energy (Fig. 7 *B*), which in turn pulls the rotor (for an arc segment *a*) in cw direction, until stator and rotor detach (Fig. 7 *C*). Their detachment is viewed as a consequence of the diverging surface geometries that lead to a rapid decrease in the electrostatic coupling forces decreasing by the square of their distance. Upon detaching, the spring relaxes and, directed by the reversal of helix rotation, the charged residues swing back into their original positions. However, due to the symmetry mismatch (Fig. 5), they land opposite an empty rotor position (Fig. 7 *D*). At this point, the springlike domain of the second stator element (the one that is in match position; see Fig. 6) takes over and pulls the rotor around for another arc segment ''b'' in an A-to-C series of steps, before the first element takes over again. This springlike device dampens the impact of discontinuous single power strokes, thus securing smoothness of rotation and prolonged attachment of the torque-generating stator elements to the rotor.

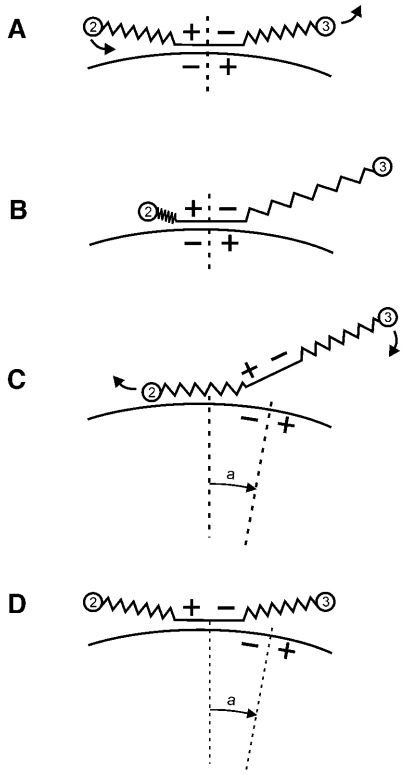

FIGURE 7 Force transmission by a mechanical spring. (*A*) The cytoplasmic MotA domain connecting transmembrane helices *2* and *3* (stator) is shown as an elastic spring (*zigzag pattern*) coupled by antipodal charges to the rotor (*arc*). The direction of helix rotation is indicated by the bent arrows. (*B*) Upon rotation of helices *2* and *3*, tension is exerted on the spring, which is used (*C*) to pull the rotor around for an arc segment ''a,'' until stator and rotor detach. (*D*) As the spring relaxes, reversed helix rotation (*curved arrows* in *C*) swings the charged residues back into the original position, however, due to the symmetry mismatch, opposite an empty position on the rotor (see Fig. 6). From here, the spring of a second stator element pulls the rotor around an equivalent amount, before the first one takes over again.

DISCUSSION

The bacterial flagellar motor is a nanomachine capable of transforming the electrochemical potential of a H^+ or a Na^+ gradient into mechanical work (torque). As long as certain fine structural and functional details of the flagellar motor remain elusive, it is a legitimate heuristic approach to propose models that account for the available empirical evidence. In the model proposed here, energy transformation involves two steps: i), the conversion of ion flow through the MotA-MotB channel into conformational changes (helix rotations) of the stator elements and ii), force transmission from the stator to the rotor by electrostatic coupling.

Two aspects of this model are new: i), The ion flow drives reversible rotational movements of transmembrane helices that form the ion channel. Helix rotation includes the cytoplasmic domain of MotA, which carries critical charged residues that mediate force transmission to the rotor by electrostatic coupling; ii), Each stator complex consists of a pair of channels, S and T, that are physically and functionally coupled. Due to their symmetry, ion flow leads to synchronous rotation of S and T. These alternate in coupling to the rotor, because of a symmetry mismatch between the interacting stator and rotor units. The proposed dynamic oscillations of the stator elements also provide a built-in mechanism for rapid motor reversal: by simply undergoing a conformational change, the rotor is able to engage the stator elements on their return strokes, thereby reversing its direction of rotation.

In classifying the model with respect to whether the ion pathway involves both the rotor and the stator, or just the stator, it clearly belongs to the second category. This contention is supported by evidence from both the H^+- and the Na^+-driven motors. First, a mutational survey of tritatable acidic residues among five proteins of the *E. coli* flagellar motor defined the conserved Asp^{32} of MotB as the only proton-binding site in the motor (Zhou et al., 1998b). This clearly favors the concept that protons flow through the

MotA-MotB channel without binding to sites on the motor. Second, upon reconstitution into proteoliposomes, the MotA-MotB analogous PomA-PomB complex of the Na^+-driven *V. alginolyticus* polar flagellar motor has been shown to catalyze the uptake of Na^+ ions (Sato and Homma, 2000). Hence, the PomA-PomB complex suffices for conducting Na^+ ions. An astounding functional homology between the H^+ and Na^+ channels was also made evident by the exchangeability of MotA and PomA and of the transmembrane portions of MotB and PomB (Asai et al., 2000). Such findings argue that the flagellar motor is an ion-driven, not strictly proton-driven, device (Berg, 1998), and that it is reasonable, therefore, to draw an analogy to the gating mechanism of the K^+ conducting KcsA channel (Perozo et al., 1999).

Reversible helix rotations (Fig. 2) that include the rotor-interactive domain(s) offer a conspicuous mechanism for torque generation, for force transmission to the rotor (Fig. 3), and for motor reversals (Fig. 6). Cyclical conformational changes in the MotA-MotB complex driven by the protonation/deprotonation of Asp^{32} (MotB) have also been proposed by Kojima and Blair (2001). Their proposal is based on small neutral substitutions of Asp^{32} that cause significant changes in the protease susceptibility of MotA. In their power-stroke model, both protonation and deprotonation contribute incrementally to the rotation of the motor. The idea of energy transformation within the stator and of conformational changes that are transmitted to the rotor is quite similar to the concept proposed here. Rather than in force transmission, charge-charge interactions have been implicated in synchronizing rotor movement and proton flux through the stator (Braun et al., 1999), a stimulating concept that accounts for tight coupling between torque and energy dissipation.

The importance of a few conserved charged residues for force transmission from the stator to the rotor was first demonstrated in a mutational survey of the MotA and FliG proteins of the H^+-driven motor of *E. coli* (Zhou et al., 1998a). It was suggested that residues Arg^{90} and Glu^{98} in the major cytoplasmic domain of MotA engage by electrostatic interactions with Arg^{281}, Asp^{288}, and Asp^{289} in the FliG C-terminal domain (Lloyd et al., 1999). In support of this concept, an analogous constellation of key functional residues—except for a Ser at the Asp^{288} position in FliG—has been experimentally defined in the ''only-cw'' rotating, H^+-driven motor of *Sinorhizobium meliloti* (U. Attmannspacher, B. Scharf, and R. Schmitt, unpublished).

The concept of force transmission by conserved charges has recently been contested by data from a mutational analysis of the Na^+-driven *V. alginolyticus* flagellar motor (Yorimitsu et al., 2002). Neutral replacements of the conserved PomA positions Arg^{88} and Glu^{96} (the homologs of Arg^{90} and Glu^{98} in MotA) do not affect motor function at high Na^+ concentration. However, at a 10-fold reduced Na^+ concentration, the mutant motor was ccw biased. Moreover, by replacing three adjacent charged residues (which are not conserved in H^+-driven motors), these authors noticed that charge reversals that include the conserved and/or the nonconserved residues rendered the motor nonfunctional. Hence, in toto these results support rather than challenge the importance of charged residues. Conceivably, the Na^+-driven motor, rotating at five times the rate of its H^+-driven homolog (Muramoto et al., 1995), requires additional charges at the stator/rotor interface for sufficient contact and efficient force transmission.

The concept of two channels in one stator complex (Fig. 4) was guided by the available biochemical evidence (Sato and Homma, 2000; Braun and Blair, 2001) and by the biophysical requirements of stator-rotor interactions (Berg, 2003). An architecture of two inversely oriented channels linked by a central homodimer of two MotB transmembrane helices was recommended by MotB cross-linking patterns and by the presence of a critical Asp^{32} residue in each of these segments. In view of only two protonatable Asp^{32} residues available, a two-channel concept appeared most plausible, although the $(MotA)_4(MotB)_2$ stoichiometry might tolerate alternative arrangements. The well-studied ion channels all have low-order symmetries ranging between twofold and fivefold (Jentsch, 2002). Therefore, a pentameric architecture was chosen, with individual channels formed by one MotB and eight MotA transmembrane helices, four inside and four outside the channel (Fig. 4). Functional transmembrane helices, namely, the MotA helices *2* and *3* adjacent to the charge-containing domain and the Asp^{32}-containing central MotB helix *5*, were positioned inside the channel; MotA helices *1* and *4* form the accessory outer frame. This concept of covalently linked inner and outer helices is similarly reflected in the molecular structure of the KcsA K^+ channel (Fig. 1; Doyle et al., 1998; Zhou et al., 2001). The overall inverse symmetry of twin channels forming the stator complex is directed by the dimer geometry of the two central MotB transmembrane helices and by the requirement for identical topologies of the two charged domains facing and contacting the rotor periphery. The given arrangement of helices makes it likely that a head-to-tail fusion of the MotA helices *4* and *1* (probably within one channel) could occur without a major loss of function, as has been reported (Sato and Homma, 2000).

The majority of known flagellar motors are able to switch and rotate at approximately the same speed in either direction (Berg, 1974). Switches occur within 10 ms in tethered cells and within 1 ms in single filaments (Kudo et al., 1990). Reversals are an inherent property of flagellar motors, but binding of a small activated response regulator (CheY-P) to the C ring increases the probability of cw over ccw rotation (Scharf et al., 1998) by switching the conformation of the C ring. In most flagellar motor models, bidirectionality is not treated explicitly. Proposed switching mechanisms involve either a change in the geometry of the rotor, or changes in the nature of interactions between protons and the motor. A

concept related to ours suggests that switching occurs as the rotor engages a different part of the stator, so that the same conformational changes of the stator drive the movement in the opposite direction (Lloyd et al., 1999). The present version considers a motor with oscillating stator complexes that provide coupling in two different planes to yield either cw or ccw rotation. By implication, while the stator is swinging back and forth, the charged MotA domain moves along a hysteresis loop and meets the rotor rim in two different planes, with one containing the antipodes matching the stator domain in forward motion. A conformational change that shifts the rotor periphery to match the return stroke of the stator elements switches the sense of rotation.

Based on KcsA ion channel dynamics and certain genetic and biochemical properties of the flagellar motor, I have proposed a new model for the mechanisms of torque generation in the stator, for force transmission and reversals of motor rotation. It predicts electrostatic force transmission in a quasi-water-free environment and elastic, springlike elements that cushion the power strokes to permit smoothness of rotation and a prolonged attachment of torque generators to the rotor. The ease with which motor reversals can be achieved by switching the match position of the rotor between forward and return strokes renders this pattern of oscillating stator elements especially attractive. Most predictions are testable using mutants with appropriate amino acid substitutions in MotA. To verify (or falsify) predictions on stator function, it will be necessary to solve the crystal structure of the MotA-MotB channel complex and to analyze its dynamics.

I thank Patrick Babinger and Klaus Stark for artwork and David Kirk for critical review. I am indebted to David Blair and Michio Homma for communicating unpublished observations and for valuable advice.

This study was supported by the Deutsche Forschungsgemeinschaft (Schm 68/34-1).

REFERENCES

Armitage, J. P., and R. M. Macnab. 1987. Unidirectional, intermittent rotation of the flagellum of *Rhodobacter sphaeroides*. *J. Bacteriol.* 169:514–518.

Armitage, J. P., and R. Schmitt. 1997. Bacterial chemotaxis: *Rhodobacter sphaeroides* and *Sinorhizobium meliloti*—variations on a theme? *Microbiology.* 143:3671–3682.

Asai, Y., I. Kawagishi, R. E. Sockett, and M. Homma. 2000. Coupling ion specificity of chimeras between H(+)- and Na(+)-driven motor proteins, MotB and PomB, in *Vibrio* polar flagella. *EMBO J.* 19:3639–3648.

Atsumi, T. 2001. An ultrasonic motor model for bacterial flagellar motors. *J. Theor. Biol.* 213:31–51.

Berg, H. C. 1974. Dynamic properties of bacterial flagellar motors. *Nature.* 249:77–79.

Berg, H. C. 1998. Keeping up with the F1-ATPase. *Nature.* 394:324–325.

Berg, H. C. 2003. The rotary motor of bacterial flagella. *Annu. Rev. Biochem.* 72:19–54.

Berg, H. C., and R. A. Anderson. 1973. Bacteria swim by rotating their flagellar filaments. *Nature.* 245:380–382.

Berg, H. C., and S. Khan. 1983. A model for the flagellar rotary motor. *In* Mobility and Recognition in Cell Biology. H. Sund and C. Velger, editors. de Gruyter, Berlin. 485–497.

Berg, H. C., and L. Turner. 1993. Torque generated by the flagellar motor of *Escherichia coli*. *Biophys. J.* 65:2201–2216.

Berry, R. M. 1993. Torque and switching in the bacterial flagellar motor. An electrostatic model. *Biophys. J.* 64:961–973.

Berry, R. M., and J. P. Armitage. 1999. The bacterial flagella motor. *Adv. Microb. Physiol.* 41:291–337.

Blair, D. F., and H. C. Berg. 1988. Restoration of torque in defective flagellar motors. *Science.* 242:1678–1681.

Block, S. M., and H. C. Berg. 1984. Successive incorporation of force-generating units in the bacterial rotary motor. *Nature.* 309:470–472.

Braun, T. F., and D. F. Blair. 2001. Targeted disulfide cross-linking of the MotB protein of *Escherichia coli*: evidence for two H(+) channels in the stator Complex. *Biochemistry.* 40:13051–13059.

Braun, T. F., S. Poulson, J. B. Gully, J. C. Empey, S. Van Way, A. Putnam, and D. F. Blair. 1999. Function of proline residues of MotA in torque generation by the flagellar motor of *Escherichia coli*. *J. Bacteriol.* 181:3542–3551.

Brown, P. N., C. P. Hill, and D. F. Blair. 2002. Crystal structure of the middle and C-terminal domains of the flagellar rotor protein FliG. *EMBO J.* 21:3225–3234.

DePamphilis, M. L., and J. Adler. 1971. Attachment of flagellar basal bodies to the cell envelope: specific attachment to the outer, lipopolysaccharide membrane and the cyoplasmic membrane. *J. Bacteriol.* 105:396–407.

Doyle, D. A., J. Morais-Cabral, R. A. Pfuetzner, A. Kuo, J. M. Gulbis, S. L. Cohen, B. T. Chait, and R. MacKinnon. 1998. The structure of the potassium channel: molecular basis of K^+ conduction and selectivity. *Science.* 280:69–77.

Elston, T. C., and G. Oster. 1997. Protein turbines. I: the bacterial flagellar motor. *Biophys. J.* 73:703–721.

Francis, N. R., V. M. Irikura, S. Yamaguchi, D. J. DeRosier, and R. M. Macnab. 1992. Localization of the *Salmonella typhimurium* flagellar switch protein FliG to the cytoplasmic M-ring face of the basal body. *Proc. Natl. Acad. Sci. USA.* 89:6304–6308.

Francis, N. R., G. E. Sosinsky, D. Thomas, and D. J. DeRosier. 1994. Isolation, characterization and structure of bacterial flagellar motors containing the switch complex. *J. Mol. Biol.* 235:1261–1270.

Götz, R., and R. Schmitt. 1987. *Rhizobium meliloti* swims by unidirectional, intermittent rotation of right-handed flagellar helices. *J. Bacteriol.* 169:3146–3150.

Hirota, N., M. Kitada, and Y. Imae. 1981. Flagellar motors of alkalophilic *Bacillus* are powered by an electrochemical potential gradient of Na^+. *FEBS Lett.* 132:278–280.

Jentsch, T. J. 2002. Chloride channels are different. *Nature.* 415:276–277.

Jones, C. J., R. M. Macnab, H. Okino, and S. Aizawa. 1990. Stoichiometric analysis of the flagellar hook-(basal-body) complex of *Salmonella typhimurium*. *J. Mol. Biol.* 212:377–387.

Khan, S., M. Dapice, and T. S. Reese. 1988. Effects of mot gene expression on the structure of the flagellar motor. *J. Mol. Biol.* 202:575–584.

Kojima, S., and D. F. Blair. 2001. Conformational change in the stator of the bacterial flagellar motor. *Biochemistry.* 40:13041–13050.

Kudo, S., Y. Magariyama, and S. Aizawa. 1990. Abrupt changes in flagellar rotation observed by laser dark-field microscopy. *Nature.* 346:677–680.

Läuger, P. 1988. Torque and rotation rate of the bacterial flagellar motor. *Biophys. J.* 53:53–65.

Lloyd, S. A., and D. F. Blair. 1997. Charged residues of the rotor protein FliG essential for torque generation in the flagellar motor of *Escherichia coli*. *J. Mol. Biol.* 266:733–744.

Lloyd, S. A., F. G. Whitby, D. F. Blair, and C. P. Hill. 1999. Structure of the C-terminal domain of FliG, a component of the rotor in the bacterial flagellar motor. *Nature.* 400:472–475.

Macnab, R. M. 1996. Flagella and motility. *In Escherichia coli* and *Salmonella*. F. C. Neidhardt, R. Curtiss III, J. L. Ingraham, E. C. C. Lin, K. B. Low, B. Magasanik, W. S. Reznikoff, M. Riley, M. Schaechter, and H. E. Umbarger, editors. ASM Press, Washington. 123–145.

Manson, M. D., P. Tedesco, H. C. Berg, F. M. Harold, and C. Van der Drift. 1977. A protonmotive force drives bacterial flagella. *Proc. Natl. Acad. Sci. USA*. 74:3060–3064.

Meister, M., G. Lowe, and H. C. Berg. 1987. The proton flux through the bacterial flagellar motor. *Cell*. 49:643–650.

Muramoto, K., I. Kawagishi, S. Kudo, Y. Magariyama, Y. Imae, and M. Homma. 1995. High-speed rotation and speed stability of the sodium-driven flagellar motor in *Vibrio alginolyticus*. *J. Mol. Biol.* 251:50–58.

Muramoto, K., S. Sugiyama, E. J. Cragoe, Jr., and Y. Imae. 1994. Successive inactivation of the force-generating units of sodium-driven bacterial flagellar motors by a photoreactive amiloride analog. *J. Biol. Chem.* 269:3374–3380.

Oosawa, F., and S. Hayashi. 1983. Coupling between flagellar motor rotation and proton flux in bacteria. *J. Phys. Soc. Jpn.* 52:4019–4028.

Perozo, E., D. M. Cortes, and L. G. Cuello. 1999. Structural rearrangements underlying K^+-channel activation gating. *Science*. 285:73–78.

Platzer, J., W. Sterr, M. Hausmann, and R. Schmitt. 1997. Three genes of a motility operon and their role in flagellar rotary speed variation in *Rhizobium meliloti*. *J. Bacteriol.* 179:6391–6399.

Ryu, W. S., R. M. Berry, and H. C. Berg. 2000. Torque-generating units of the flagellar motor of *Escherichia coli* have a high duty ratio. *Nature*. 403:444–447.

Samuel, A. D., and H. C. Berg. 1995. Fluctuation analysis of rotational speeds of the bacterial flagellar motor. *Proc. Natl. Acad. Sci. USA*. 92:3502–3506.

Sato, K., and M. Homma. 2000. Functional reconstitution of the Na(+)-driven polar flagellar motor component of *Vibrio alginolyticus*. *J. Biol. Chem.* 275:5718–5722.

Scharf, B. E., K. A. Fahrner, L. Turner, and H. C. Berg. 1998. Control of direction of flagellar rotation in bacterial chemotaxis. *Proc. Natl. Acad. Sci. USA*. 95:201–206.

Schmitt, R. 2002. Sinorhizobial chemotaxis: a departure from the enterobacterial paradigm. *Microbiology*. 148:627–631.

Schrempf, H., O. Schmidt, R. Kummerlen, S. Hinnah, D. Muller, M. Betzler, T. Steinkamp, and R. Wagner. 1995. A prokaryotic potassium ion channel with two predicted transmembrane segments from *Streptomyces lividans*. *EMBO J.* 14:5170–5178.

Silverman, M., and M. Simon. 1974. Flagellar rotation and the mechanism of bacterial motility. *Nature*. 249:73–74.

Sosinsky, G. E., N. R. Francis, D. J. DeRosier, J. S. Wall, M. N. Simon, and J. Hainfeld. 1992. Mass determination and estimation of subunit stoichiometry of the bacterial hook-basal body flagellar complex of *Salmonella typhimurium* by scanning transmission electron microscopy. *Proc. Natl. Acad. Sci. USA*. 89:4801–4805.

Thomas, D. R., D. G. Morgan, and D. J. DeRosier. 1999. Rotational symmetry of the C ring and a mechanism for the flagellar rotary motor. *Proc. Natl. Acad. Sci. USA*. 96:10134–10139.

Thomas, D. R., D. G. Morgan, and D. J. DeRosier. 2001. Structures of bacterial flagellar motors from two FliF-FliG gene fusion mutants. *J. Bacteriol.* 183:6404–6412.

Walz, D., and S. R. Caplan. 2000. An electrostatic mechanism closely reproducing observed behavior in the bacterial flagellar motor. *Biophys. J.* 78:626–651.

Yorimitsu, T., S. Yoshiyuki, A. Ishijima, T. Yakushi, and M. Homma. 2002. The conserved charged residues in the cytoplasmic loop of the Na^+-driven flagellar motor component PomA in *Vibrio alginolyticus*. *J. Mol. Biol.* 320:403–413.

Zhou, J., S. A. Lloyd, and D. F. Blair. 1998a. Electrostatic interactions between rotor and stator in the bacterial flagellar motor. *Proc. Natl. Acad. Sci. USA*. 95:6436–6441.

Zhou, J., L. L. Sharp, H. L. Tang, S. A. Lloyd, S. Billings, T. F. Braun, and D. F. Blair. 1998b. Function of protonatable residues in the flagellar motor of *Escherichia coli*: a critical role for Asp 32 of MotB. *J. Bacteriol.* 180:2729–2735.

Zhou, Y., J. H. Morais-Cabral, A. Kaufman, and R. MacKinnon. 2001. Chemistry of ion coordination and hydration revealed by a K+ channel-Fab complex at 2.0 A resolution. *Nature*. 414:43–48.